European Journal of Orthodontics, 2022, **44**, 690–697
https://doi.org/10.1093/ejo/cjac041
Advance Access publication 18 August 2022
Original Article

Periodontal ligament cells derived small extracellular vesicles are involved in orthodontic tooth movement

Yimei Zhang[1], Ting Zhang[2,3,4], Ziqian Zhang[5], Junxiang Su[5], Xiaowen Wu[5], Liyuan Chen[2,3,4], Xuejun Ge[5], Xiujing Wang[1] and Nan Jiang[3,4,6]

[1]First Clinic Division, Peking University Hospital of Stomatology, Beijing, PR China
[2]Laboratory of Biomimetic Nanomaterials, Department of Orthodontics, Peking University School and Hospital of Stomatology, Beijing, PR China
[3]National Engineering Laboratory for Digital and Material Technology of Stomatology, Peking University School and Hospital of Stomatology, Beijing, PR China
[4]Beijing Key Laboratory of Digital Stomatology, Peking University School and Hospital of Stomatology, Beijing, PR China
[5]Department of Endodontics, Shanxi Medical University School and Hospital of Stomatology, Shanxi, PR China
[6]Central Laboratory, Peking University School and Hospital of Stomatology, Beijing, PR China

Correspondence to: Xiujing Wang, First Clinic Division, Peking University Hospital of Stomatology, 37# Xishiku Jia, Xicheng District, Beijing 100034, PR China.
E-mail: wang_xiu_jing@163.com
Nan Jiang, Central Laboratory, Peking University School and Hospital of Stomatology, National Engineering Laboratory for Digital and Material Technology of Stomatology, Beijing Key Laboratory of Digital Stomatology, 22# Zhongguancun South Avenue, Haidian District, Beijing 100081, China.
E-mail: nanjiang@bjmu.edu.cn

Summary

Objectives: Small extracellular vesicles (EVs) from human periodontal ligament cells (hPDLCs) are closely associated with periodontal homeostasis. Far less is known about EVs association with orthodontic tooth movement (OTM). This study aimed to explore the role of small EVs originated from hPDLCs during OTM.

Materials and methods: Adult C57BL/6 mice were used. Springs were bonded to the upper first molars of mice for 7 days to induce OTM *in vivo*. To block small EVs release, GW4869 was intraperitoneally injected and the efficacy of small EVs inhibition in periodontal ligament was verified by transmission electron microscope (TEM). Tooth movement distance and osteoclastic activity were studied. *In vitro*, hPDLCs were isolated and administered compressive force in the EV-free culture media. The cell morphologies and CD63 expression of hPDLCs were studied. Small EVs were purified and characterized using a scanning electron microscope, TEM, western blot, and nanoparticle tracking analysis. The expression of proteins in the small EVs was further processed and validated using a human immuno-regulated cytokines array and an enzyme-linked immunosorbent assay (ELISA).

Results: The small EV depletion significantly decreased the distance and osteoclastic activity of OTM in the mice. The hPDLCs displayed different morphologies under force compression and CD63 expression level decreased verified by western blot and immunofluorescence staining. Small EVs purified from supernatants of the hPDLCs showed features with <200 nm diameter, the positive EVs marker CD63, and the negative Golgi body marker GM130. The number of small EVs particles increased in hPDLCs suffering force stimuli. According to the proteome array, the level of soluble intercellular adhesion molecule-1 (sICAM-1) displayed the most significant fold change in small EVs under compressive force and this was further confirmed using an ELISA.

Limitations: Further mechanism studies are warranted to validate the hPDLC-originated small EVs function in OTM through proteins delivery.

Conclusions: The notable decrease in the OTM distance after small EV blocking and the significant alteration of the sICAM-1 level in the hPDLC-originated small EVs under compression provide a new vista into small EV-related OTM biology.

Introduction

Orthodontic tooth movement (OTM) may be considered a regional inflammatory process that is characterized by alveolar bone and periodontal ligament (PDL) remodelling (1). Human periodontal ligament cells (hPDLCs) are the predominant cell type in connective tissue around teeth, and they sense and respond to mechanical stimuli (2). In many studies, secreted factors of hPDLCs have been shown to be involved in inflammation and also in periodontal regeneration (2,3). Abundant inflammatory cytokines are released by hPDLCs into the gingival crevicular fluid (GCF) and the periodontal environment, recruiting immune cells that regulate regional bone metabolism (4). However, little has been revealed about the secreted factors other than cytokines are released by hPDLCs under mechanical stress.

Extracellular vesicles (EVs) are particles that are naturally released from cells, which are delimited by a lipid bilayer but cannot replicate due to the lack of a functional nucleus. Small EVs are vesicles with diameters <200 nm, previously generalized as exosomes, that can be secreted by nearly all cell types to most body fluids (5). Small EVs embody bioactive molecules, such as proteins, lipids, and nucleic acids, including

mRNA and non-coding RNA, transmitting information between cells and functioning in physiological, pathological, and therapeutic processes (6). A wide range of studies have illuminated their role in the crosstalk between stimuli and the immune response, for example, myocardial ischemia, repercussion injury, wound healing, graft-versus-host-disease, and bone and cartilage regeneration (6–8). Recent studies have demonstrated that the small EVs released by hPDLCs are enhanced by lipopolysaccharide (LPS) treatment and involved in inflammatory signalling that influences bone remodelling. This indicates that small EVs released by hPDLCs might play a pivotal role in regulating the periodontal environment (9).

Preliminary work has been conducted to investigate cyclic stretch force stimulations of hPDLCs, and this work has suggested that anti-inflammatory small EVs are released by force stimulated hPDLCs. This process might contribute to the maintenance of periodontal immune/inflammatory homeostasis. In contrast to the increase of inflammatory interleukin 1 beta (IL-1β) level under mechanical stimuli, as reported in previous studies, force-induced hPDLCs release small EVs that inhibit IL-1β production in LPS/nigericin-stimulated macrophages by inhibiting the nuclear factor kappa B (NF-κB) signalling pathway (10). Such results indicate that the role of small EVs from hPDLCs cells and their clinical significance in OTM need to be elucidated.

The purpose of this study is to investigate the following: (1) the role of PDL derived small EVs in a mouse OTM model, to potentially explain the orthodontic clinical significance of small EVs and (2) the change in the candidate chemokines and cytokines in hPDLC-derived small EVs, to explore small EV protein alterations under mechanical stimuli, which offer a new understanding of the biology of OTM.

Materials and methods

Animals and treatments

Adult C57BL/6 mice (20–25 g, 7–8 weeks, male, Weitong Lihua Experimental Animal Center, Beijing, China) were used in the study to evaluate small EV functions during OTM. Briefly, the mice were anaesthetized using intraperitoneally injection with pentobarbital sodium (100 mg/kg) prior to surgery. Mechanical force was then applied following a previously published method (11,12). A nickel-titanium coil spring (0.2 mm in wire size, 1 mm in diameter, and 1 mm in length; Smart Technology) was bonded between the maxillary right first molar and incisors by 30 g of the coiled spring for seven days. The contralateral first molar was used as the blank control. The mice were divided into two groups, namely, the control group with the force application and 0.005% dimethyl sulfoxide (DMSO) and the treatment group with force application and 0.005% GW4869. A pilot study was conducted to estimate the total sample size to detect the overall difference between the control group and the treatment group. Based on an α-level of 0.05 and a desired power (1 – β) of 0.90, the total sample size was estimated to be 18 (nine mice in each group). Eighteen mice were randomly allocated to two groups, while the control group received 0.005% DMSO, and the treatment group received 0.005% GW4869 diluted in DMSO during OTM.

According to previous studies, the neutral sphingomyelinase (nSMase) inhibitor, GW4869, reduces small EV release (13,14). Thus, GW4869 (Merck, Darmstadt, Germany) was dissolved and diluted in DMSO (Merck, Darmstadt, Germany) to make a final concentration of 0.005%. The drug was maintained at 4°C for up to one week prior to use. The GW4869 work solution was intraperitoneally injected daily into the OTM mice at a dose of 1 μg/g for the first five consecutive days. The same volume of a 0.005% DMSO buffer was injected as the control. The animals were euthanized by carbon dioxide inhalation followed by cervical dislocation. After euthanizing, the maxilla of each animal was then dissected and fixed in 10% formalin (Figure 1A). All of the experimental procedures involving the C57BL/6 mice were approved by the Animal Use and Care Committee of Peking University (protocol number: LA2021226).

Measurement of the tooth movement distance

The occlusal view of the maxilla was recorded using a stereomicroscope (SWZ1000; Nikon, Japan). The OTM distance was measured using a modified method as previously described (12). The amount of OTM was determined by measurement between the most convex points of the distal surface of the first molar and the mesial surface of the second molar. Measurements were first conducted by two investigators (TZ and ZnZ) who were blinded to the groups, and the intra-correlation coefficient (ICC) for intra-examiner agreement was 0.91. All of the measurements were then repeated after 2 weeks by TZ and ICC for inter-examiner error was 0.95. The average of the two measurements by TZ was used in the evaluation.

Periodontal ligament transmission electron microscope

The maxillary right first molar was sectioned gently using forceps. The PDL tissues, which were scraped from the surfaces of each dental root using a scalpel, were immersed in a mixture of phosphate-buffered saline (PBS) with 2% paraformaldehyde, 2% glutaraldehyde, and 0.5% $CaCl_2$ for 24 h at 4°C. The tissues were dehydrated in a series of graded ethanol solutions and then embedded in a mixture of nadic methyl anhydride, dodecenyl succinic anhydride, and tridimethyl aminomethyl phenol. The slides were sectioned at a thickness of 80 nm, and the obtained samples were double-stained with 6% uranyl acetate and lead citrate. Images were obtained using a transmission electron microscope (TEM) operating at 80 kV (JEM-1400, Japan) (15).

Tartrate-resistant acid phosphatase staining

The transverse serial sections (4.5 μm) from the corresponding group were stained for tartrate-resistant acid phosphatase (TRAP) using a leukocyte acid phosphatase kit (387A, Sigma, Saint Louis, Missouri, USA) according to the manufacturer's protocol. The mesial periodontal site of the distal-buccal root of the first molar was used for the osteoclasts counts. The TRAP positive multinucleated cells that attached to the alveolar bone surface were counted (n = 5). The slides were evaluated by two examiners who were blinded to the group status (11).

Cell culture

In this study, we obtained human periodontal tissue samples by following protocols approved by Ethics Committee of Peking University (protocol number: PKUSSIRB-201311103) with appropriate informed consent. The hPDLCs were isolated from the periodontal ligament of healthy bicuspids extracted due to

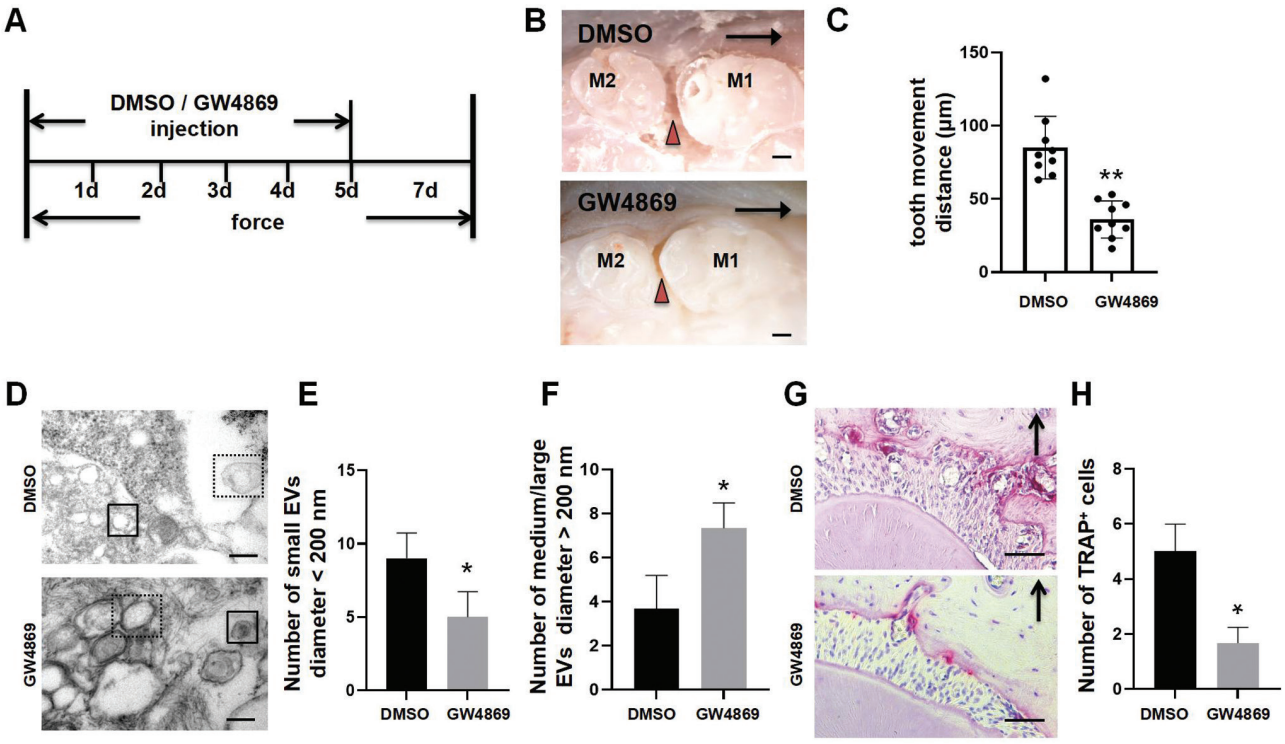

Figure 1. Effect of blocking small EVs in mice by GW4869 injection during OTM. (A) Flow chart of the experiment. Orthodontic force was applied to mice in two groups for 7 days. The injection of GW4869 or DMSO was performed for five consecutive days since day one. (B) The representative images of the occlusal view of the first and second molars after OTM in mice. M1, the first molar. M2, the second molar. The The triangle arrowheads indicate the measurement of the OTM distance. The black arrows show the direction of force application (scale bar = 100 μm). (C) Statistical results of the tooth movement distance in the two groups. The OTM distance significantly decreased in the GW4869-injected group comparing to the DMSO-injected group (n = 9; $^{**}P < 0.01$). (D) TEM images of the representative area of periodontal ligament in the GW4869-injected group compared to the DMSO-injected group. (The solid line box showed representative small EVs with diameters < 200 nm. The dotted line box showed medium/large EVs > 200 nm; Scale bar = 200 nm.). (E) Semi-quantification of the number of small EVs with diameters < 200 nm. (n = 5; $^{*}P < 0.05$). (F) Semi-quantification of the number of medium/large EVs with diameters > 200 nm (n = 5; $^{*}P < 0.05$). (G) Representative TRAP staining images on the compression side of distal-buccal root of M1. The arrow showed the direction of orthodontic force (scale bar = 50 μm). (H) The number of TRAP-positive cellsosteoclasts decreased after being treated by GW4869 injections (n = 5; $^{*}P < 0.05$). *DMSO*, dimethyl sulfoxide, extracellular vesicles; *EVs*, extracellular vesicles; *OTM*, orthodontic tooth movement; *TEM*, transmission electron microscope; *TRAP*, tartrate-resistant acid phosphatase.

orthodontic treatment as previously described (16). The hPDLCs were cultured with alpha modification of Eagle's medium containing 15% foetal calf serum (GIBCO, Carlsbad, California, USA), 100 U/ml penicillin, and 100 g/ml streptomycin (Biofluids, Rockville, Maryland) and incubated at 37°C in a 5% carbon dioxide atmosphere. The hPDLCs were used at passage four according to our published protocols (11,12). A light inverted microscope was used to observe the alignments and shapes of the cultured hPDLCs. Mechanical stimuli were applied on the cultured hPDLCs as previously described (11,12,17). Briefly, a glass cover with 1 g/cm^2 metal weights on top was placed over an 80% confluent cell layer in six-well plates to exert a continuous compressive force for 6 h, 12 h, and 24 h.

Immunofluorescence staining

Immunofluorescence staining was performed according to a previous study (18). Briefly, the hPDLCs were cultured with or without 1 g/cm^2 of compressive force for 24 h. The treated hPDLCs were washed with PBS and fixed using a 4% paraformaldehyde fixative. The cells were subsequently stained with anti-CD63 antibodies (1:500 dilution; Abcam) and Alexa Fluor 488 Phalloidin for staining F-actin (green fluorescence; 1:200; Millipore Sigma, Saint Louis, Missouri, USA). Stained sections were then incubated with tetramethylrhodamine isothiocyanate-conjugated secondary antibody (red fluorescence; 1:200, Jackson Immuno Research Laboratories, West Grove, Pennsylvania, USA) to identify CD63. The nuclei were counterstained with 4′,6-diamidino-2-phenylindole (blue fluorescence; 1:200; Millipore sigma, Saint Louis, Missouri, USA). Images were acquired using a Zeiss laser scanning microscope (LSM 510; Jena, Germany) and processed using LSM 5 Release 4.2 software.

Western blot

Western blotting was performed as previously described in detail (18). The total protein was extracted from the cultured cells and small EVs using the RIPA lysis buffer (Sigma Aldrich) with a protein inhibitor cocktail (Roche, USA) and the PhosSTOP phosphatase inhibitor cocktail (Roche, USA). The lysates were then centrifuged at 12 000 g for 15 min. The supernatants were collected for further use. The proteins were separated using 10% SDS-PAGE, transferred onto a polyvinylidene fluoride membrane (Bio-Rad), blocked in 5% BSA, and then probed overnight with primary antibodies, including CD63 (1:1000; Systembio, Palo Alto, USA) and GM130 (1:1000; Abcam, Cambridge, UK). The blots were then incubated with horseradish peroxidase-conjugated secondary antibodies (1:5000; Zhongshan Golden Bridge Biotechnology, Beijing, China). Finally, the protein bands

were enhanced by chemiluminescence detection prior to being photographed.

Small EVs isolation and nanoparticle tracing analysis

The hPDLCs culture supernatants were centrifuged at 300 g for 10 min. The supernatant was collected and centrifuged at 2000 g for 10 min, and this was followed by centrifugation at 10 000 g for 60 min. The final supernatant was then ultracentrifuged (Beckman Coulter, USA) at 100 000 *g* for 70 min. The pellet was washed in a large volume of PBS to eliminate contamination of proteins and centrifuged at 100 000 *g* for another 70 min. The collected vesicles from the hPDLCs were resuspended in PBS and characterized by ZetaView 8.04.02 SP2 (Particle Metrix, Meerbusch, Germany) (19,20).

Transmission and scanning electron microscopy for small EVs

The small EVs were fixed in 2% paraformaldehyde, mixed gently, and loaded onto Formvar-carbon-coated grids in a dry environment for 20 min. The samples were then contrasted in 2% phosphotungstic acid for 2 min. Samples were washed, dried, and examined using an electron microscope (JEM-1400, Japan). For SEM, the small EVs were fixed in 2% paraformaldehyde and examined using a scanning electron microscope according to a previous study (19,20).

Protein array

The small EVs obtained from the cell culture medium of the hPDLCs from three biological replicates were pooled and further quantified using BCA. A total of 20 μg of protein from each group was processed by two technical repeats to a proteome profiler™ human cytokine array, panel A according to the instructions (R&D Systems, Minnesota, USA) for 36 inflammatory human cytokines.

Enzyme-linked immunosorbent assay

The concentration of sICAM-1 in small EVs was measured using a Human sICAM-1 enzyme-linked immunosorbent assay (ELISA) Kit (Beijing 4A Biotech Co., Ltd., China) according to the manufacturer's instructions. Briefly, 1 μg of small EV protein from each group was added to 96-well plates coated with a mouse anti-human sICAM-1 antibody and incubated at room temperature for 1 h. After washing, the wells were incubated with streptavidin-peroxidase-conjugated anti-mouse IgG Ab at room temperature for 1 h. All of the unbound material was washed away, and a peroxidase enzyme substrate was added. The colour development was stopped and the intensity of the colour was measured.

Data analysis and statistics

We used a descriptive analysis to summarize the data of the OTM. The statistical analysis was performed using SPSS 19.0 for Windows (SPSS, Inc.). The normal distribution of the raw data was confirmed using a one-sample Kolmogorov-Smirnov test. Comparisons between the two groups were analysed using independent unpaired two-tailed Student's *t*-tests. $P < 0.05$ was considered to be statistically significant. All of the data are presented as mean ± SD. The intra-examiner reliability was measured using Cohen's kappa, and it was > 0.9 for all measurements. We based the selected sample size for the *in vivo* experiment on a pilot study for an α value of 0.05 and the statistical methods β value of 0.1. We determined the sample size for the *in vivo* studies to be nine.

Results

Reduced distance of tooth movement in the GW4869-treated mice

To investigate whether small EVs participate in the process of OTM, we used a mouse OTM model according to previous studies (11,12). Mice were injected daily with 0.005% GW4869 or DMSO for five consecutive days and applied mechanical force for seven days prior to being sacrificed (Figure 1A). The OTM distance (triangle arrowhead) in the force applied side of the DMSO-injected group resulted in 85.11 ± 21.38 μm, whereas the OTM distance in the GW4869-injected group was significantly decreased to 36.00 ± 12.47 μm (Figure 1B and C; Table 1). TEM results of the periodontal ligament tissue showed a significant decrease in the number of small EVs (solid line box, <200 nm) and a significant increase in the medium/large EVs (dotted line box, >200 nm) in the GW4869-injected group (Figure 1D–F) in concordance with the reported GW4869 impact on the EV population (21). We further showed that blocking small EVs repressed osteoclastic activity on the compression side of PDL and alveolar bone (Figure 1G and H), which may contribute to the decrease of tooth movement distance.

Static compressive force induced the secretion of small EVs from hPDLCs

Regarding the predominant role of hPDLCs for sensing and responding to mechanical stimuli, we further explored the small EV release of hPDLCs in an *in vitro* model. The hPDLCs were isolated and were given 1 g/cm^2 of static compression per our prior methods and cultured in an EV-free media (Figure 2A). The compressed hPDLCs displayed different morphology and cytoskeletons under the mechanical stimuli. A loosening of the aligned cell connection but elongation of the cell body distribution were observed, compared with the control group (Figure 2B). We also showed a decreased signal of CD63 in hPDLCs in the force group by immunofluorescence staining (Figure 2C). Further western blot of a time-course force application on hPDLCs was performed and quantified, showing the decreased expression of

Table 1. Distribution of OTM distance measurement (μm) in DMSO and GW4869 groups.

DMSO	GW4869
83	50
80	30
132	30
103	23
66	33
76	16
63	53
90	43
73	46

DMSO, dimethyl sulfoxide; OTM, orthodontic tooth movement.

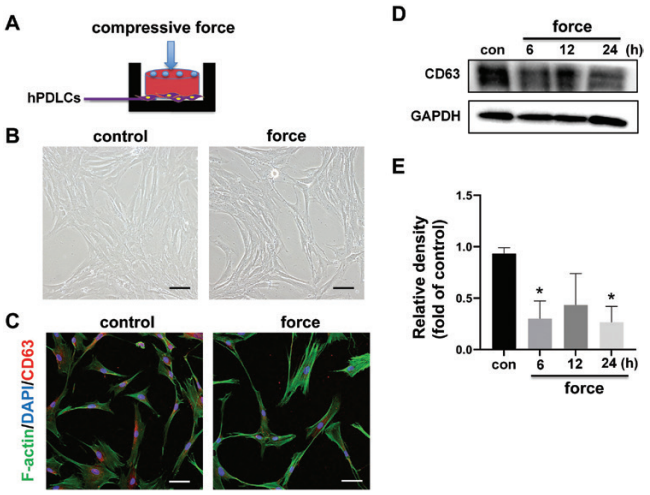

Figure 2. hPDLCs characterization under compressive force. (A) Graphic scheme of compressive force application. (B) Light microscope images of the hPDLCs alignment patterns in two groups (scale bar = 100 μm). (C) Immunofluorescence staining of CD63 and phalloidin in hPDLCs (scale bar = 100 μm). (D, E) The western blot of a time-course force application quantified the decrease expression of CD63 in the force group compared to the control group ($n = 3$; $^*P < 0.05$). hPDLCs, human periodontal ligament cells.

CD63 in force group compared to control group (Figure 2D and E).

For further characterization, small EVs purified from the supernatant of hPDLCs from the control and compressive force group were verified using SEM (Figure 3A) and TEM (Figure 3B), showing that the diameters of the small EVs were <200 nm, which is consistent with the characterization of the small EV sizes in previous studies (5,6). The isolated small EVs from the control and the compressive force groups in the hPDLCs were further processed using a western blot analysis. As shown in Figure 3C, the expression of the small EV marker CD63 was positive, but the expression of Golgi body maker GM130 was negative. This result suggested the absence of Golgi or cell contamination in both groups. The nanoparticle tracing analysis (NTA) revealed the distribution of vesicles with diameters of 122.7 ± 43.6 nm in the control group and with diameters of 118.4 ± 47.8 nm in the force group (Figure 3D). The NTA results also showed 1.6×10^9 small EVs were released by 10^6 hPDLCs in the 24 h EV-free culture media versus 2.1×10^9 small EVs released by the same number of hPDLCs in the 24h EV-free culture media under compressive force.

Decrease of sICAM-1 in small EVs from hPDLCs subjected to compressive force

To explore the possible small EVs content changes in the compressed hPDLCs, we used a cytokine array to perform semi-quantification of 36 inflammatory cytokines in the small EVs extracted from the cell culture supernatant of both control and 1g/cm^2 static compression hPDLCs for 24 h. Eight cytokines were detected in the exosomes from control cells and the hPDLCs subjected to compressive force. Of the cytokines, CXCL1 and IL-13 were up-regulated, and six cytokines, IFN-γ, CD40 ligand, Serpin E15, MIF, IL-23, and sICAM-1, were down-regulated after the compressive force application (Figure 4A and B). To validate the array results, we further performed an ELISA test for sICAM-1 that showed the most remarkable change. sICAM-1 displayed a significant decreasing tendency in small EVs from the compressed hPDLCs that was consistent with the array data (Figure 4C).

Discussion

Recent studies have presented reports regarding small EVs (particularly exosomes) that play important roles in localized periodontal inflammation and repair (9,10). Thus, we were prompted to study whether small EVs participate in OTM. First, we observed the *in vivo* phenomena that systemic inhibition of small EVs in mice led to decreasing release of small EVs in PDL, significantly reduced OTM distance and osteoclastic activity. Second, we explored the mechanism of animal results by *in vitro* experiments on hPDLCs under compressive stimuli. hPDLCs, as predominant cell type subjected to mechanical stimuli in periodontal tissue, were isolated and administered static compression. The deformed alignment and cell body distribution were observed in the hPDLCs under compressive force. Decrease expression of CD63 was also detected in hPDLCs under force application. Small EVs purified from the supernatant of hPDLCs were characterized and further quantified with increase particles number after force application. Third, the immune-regulated cytokine expressions in the small EVs from the hPDLCs under force stimuli were explored, and the sICAM-1 displayed a significant decreasing tendency. These data suggested that periodontal ligament-related small EVs were involved in OTM, and immune-related proteins, such as sICAM-1, may have played an important role.

Mechanical stimuli are prevailing in a physiological periodontal environment. The periodontal ligament is exposed to mechanical loading, such as tension, compression, fluid shear, and hydrostatic force, produce various components to regulate signals for the remodelling of periodontal tissue (10). However, our understanding of the mechanical-chemical transduction process remains incomplete, and this may contribute to unsolved clinical problems such as the unexpected prolonged treatment time in some populations, unwanted clinical results such as iatrogenic root resorption or trauma-related ankylosis (22,23). In addition, the optimal force may also lead to the repair and rebuilding of periodontal tissue in severe periodontitis cases that are combined with proper periodontal treatment (24). The mechanism behind such clinical phenomena is worthy of study. Apart from biological molecules, such as ILs, tumour necrosis factors (TNFs), interferons (IFNs), growth factors, and colony-stimulating factors (CSFs) that directly secrete into the periodontal environment, novel secretome elements in the PDL were discovered and proven to be of clinical significance in OTM (25,26). In this study, we explored small EVs in a mouse OTM model by controlling small EVs release. We demonstrated a decrease in OTM distance and inhibited osteoclastic activity. Our results were consistent with previous studies, that small EVs might play a role in periodontal fibroblast-to-osteoblast communication under inflammatory stimuli (27–29). Due to the limitation of drug administration, EVs deletion could not be specified to periodontal ligament cells. Precise deletion of EVs in periodontal tissue would be a more powerful animal model to elucidate mechanisms.

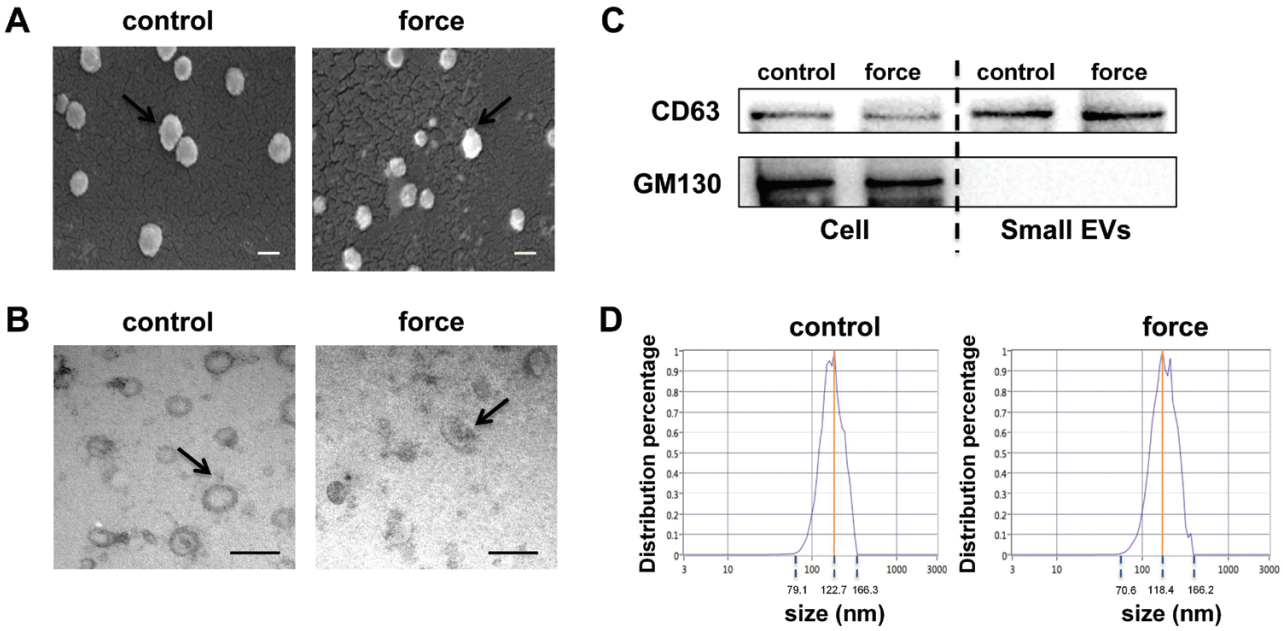

Figure 3. Characterization of small EVs derived from hPDLCs under compressive force. (A) Scanning electron microscopy and (B) Transmission electron microscopy showed extracellular vesicles isolated from both groups (scale bar = 100 nm). (C) Expression of CD63 and GM130 from the vesicles and cells were detected via western blot. (D) The NTA analysis revealed the distribution of vesicles in the control group and the force group. *EVs*, extracellular vesicles; *hPDLCs*, human periodontal ligament cells; *NTA*, nanoparticle tracing analysis.

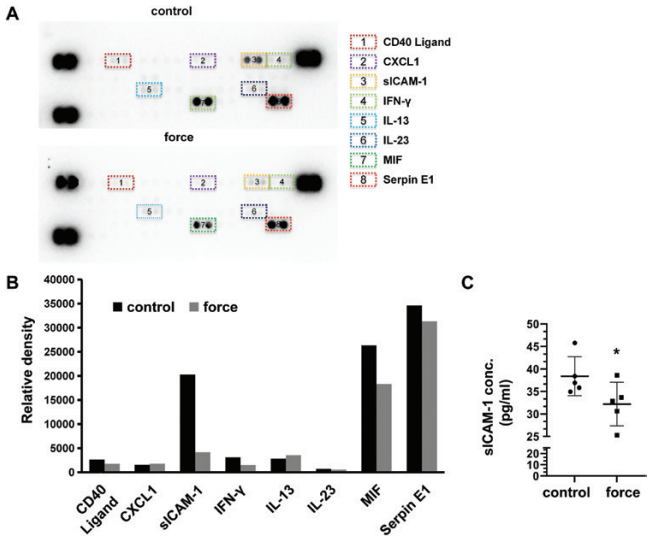

Figure 4. Inflammatory cytokine profile of the small EVs released by the hPDLCs under compressive force. (A) Proteome profile human cytokine array of the small EVs isolated from the hPDLCs with or without compression force. The pixel intensity of the spots was measured, and the relative abundance was adjusted to the background and visualized as a graph. (B) The pixel intensity of eight cytokines. (C) The expression of sICAM-1 tested by ELISA ($n = 5$; $^*P < 0.05$). *EVs*, extracellular vesicles; *hPDLCs*, human periodontal ligament cells; *ELISA*, enzyme-linked immunosorbent assay

Small EVs, often referred to as 'exosomes' in previous studies, are spherical vesicles with diameters <200 nm, and they are enriched in biological molecules. Small EVs have been studied as novel communication packages between cells (5,6,8). The extensive roles of small EVs have been reported in the periodontal environment (9,10). It has been reported that exosomal microRNA-155-5p from periodontal ligament stem cells influences the progress of chronic periodontitis by regulating the Th17/Treg balance (27). Moreover, another study showed that mesenchymal stem cell-derived small EVs repaired periodontal defects by regenerating periodontal tissues, including newly formed bone and periodontal ligament (28). However, our understanding of their role in the mechanical-chemical transduction process in OTM remains incomplete. Therefore, with our result from the *in vivo* OTM study, we further explored small EVs release in hPDLCs, which are the dominant cells that respond to mechanical stimuli in a periodontal environment. We studied the characterization of EVs both in cells and secretion forms from hPDLCs under compression. In hPDLCs under compression, deformed alignment of cells and decreasing expression of CD63 were observed. We further extracted small EVs from hPDLCs in the model, identified spherical vesicles with diameter <200 nm, enriched in CD63. We also showed increasing release of small EVs by hPDLCs under force stimuli. Based on previous studies, CD63 is a ubiquitously expressed protein that is localized within the endosomal system and at the cell surface. In late endosomes, CD63 is enriched on the intraluminal vesicles, which by specialized cells are secreted as exosomes through fusion of endosomes with the plasma membrane (30). Our result indicated force application influenced small EVs trafficking and release in hPDLCs.

Considering small EVs serve as modulators of cell-to-cell communication and can effectively protect contents from the extracellular environment for specific delivery to recipient cells. We further focused on mechanical loading on small EVs proteins changes. Small EVs contain a broad array of transmembrane proteins, lipid-anchored membrane proteins, peripherally associated membrane proteins, and soluble proteins of the exosome lumen (5). On the basis of previous reported inflammatory cytokines extracted from mechanical stimulated hPDLCs culture medium, we performed immunoregulated proteins array in hPDLCs small EVs. Among these candidate proteins, ILs, TNFs, IFNs, and CSFs have

been reported extensively expressed in GCF or culture medium from hPDLCs related to mechanical stimuli (31–34). However, our study discovered a significant decrease of sICAM-1, which is a spliced isoform of ICAM-1, truncated at the transmembrane domain but retains extracellular Ig domains (35). In periodontal environment, sICAM-1 was reported as a biomarker of periodontitis prognosis, indicating inflammation or wound healing after clinical treatment (36). Both ICAM-1 and sICAM-1 are reported of great importance in regulating immune cells. Different outcome of the sICAM-1 interactions with receptors depending on its concentration and conformation. Low levels of sICAM-1 are proved to activate NF-κBand ERK, leading to the release of inflammatory cytokines such as macrophage inflammatory protein (MIP)-1a, MIP-2. On contrary, high levels of sICAM-1 competitively interfered leukocyte interactions and angiogenesis, promoting pro-repair activity of immune cells (37). Furthermore, membranous form of ICAM-1 (mICAM-1) was reported to be associated with small EVs of cancer cells, exhibits potent immune modulatory activity (38). Also, Exosomal ICAM-1 from mature dendritic cells plays critical role in T-cell priming (38). In our present data, expression of sICAM-1 in small EVs decreased significantly in hPDLCs subjected to compressive force, indicating possible downstream response of immune cells such as macrophage and T cells, which have been reported involved in OTM (39,40). However, the mechanism and function of small EVs sICAM-1 changes in hPDLCs warranted further confirmation.

In all earnestness, the present work should be viewed upon as preliminary. Further work is required to investigate whether compressive force-induced hPDLCs small EVs influence immune cells through sICAM-1 delivery in OTM biology. Potential gene components, such as miRNAs and other non-coding RNAs, from small EVs, need to be verified under force stimuli. Moreover, we should also investigate the possible clinical application of hPDLCs-derived small EVs in OTM-related pathology.

Conclusions

In summary, this study concludes that (1) the mouse OTM distance and osteoclastic activity were hampered by blocking small EVs, thus potentially explaining the functional significance of small EVs; and (2) the compressive force altered small EVs released by the hPDLCs, the predominant cell type that responded to mechanical stimuli, showing a decreasing tendency of sICAM-1. In addition, the periodontal ligament cell-derived EVs could be considered to have great significance in the paracrine pathway of OTM.

Acknowledgements

The authors wish to thank Mr Liu Zhihua for his support in creating the illustrations.

Funding

The authors acknowledge the financial support from the projects of the National Natural Science Foundations of China nos. 81801014, 81970901, 82170996, the Beijing Nova Program no. Z201100006820080, and the Peking University Hospital of Stomatology New Clinical Technology no. PKUSSNCT-13A11.

Conflicts of interest

No authors hold a conflict of interest to declare regarding this study.

Authors' contributions

YZ performed the *in vitro* experiments, analysed the data, and prepared the manuscript. TZ, ZZ, JS, and XW performed the *in vivo* experiments. LC performed the western blot experiments. XG, XW, and NJ designed the experiments and revised the manuscript.

Data availability

The data underlying this article will be shared on reasonable request to the corresponding author.

References

1. Masella, R.S. and Meister, M. (2006) Current concepts in the biology of orthodontic tooth movement. *American Journal of Orthodontics and Dentofacial Orthopedics*, 129, 458–468.
2. Garlet, T.P., Coelho, U., Silva, J.S. and Garlet, G.P. (2007) Cytokine expression pattern in compression and tension sides of the periodontal ligament during orthodontic tooth movement in humans. *European Journal of Oral Sciences*, 115, 355–362.
3. Krishnan, V. and Davidovitch, Z. (2009) On a path to unfolding the biological mechanisms of orthodontic tooth movement. *Journal of Dental Research*, 88, 597–608.
4. Meikle, M.C. (2006) The tissue, cellular, and molecular regulation of orthodontic tooth movement: 100 years after Carl Sandstedt. *European Journal of Orthodontics*, 28, 221–240.
5. Théry, C., *et al.* (2018) Minimal information for studies of extracellular vesicles 2018 (MISEV2018): a position statement of the International Society for Extracellular Vesicles and update of the MISEV2014 guidelines. *Journal of extracellular vesicles*, 7, 1535750.
6. Théry, C., Ostrowski, M. and Segura, E. (2009) Membrane vesicles as conveyors of immune responses. *Nature Reviews Immunology*, 9, 581–593.
7. Xu, L., Geng, T., Zang, G., Bo, L., Liang, Y., Zhou, H. and Yan, J. (2020) Exosome derived from CD137-modified endothelial cells regulates the Th17 responses in atherosclerosis. *Journal of Cellular and Molecular Medicine*, 24, 4659–4667.
8. Xu, R., Greening, D.W., Zhu, H.J., Takahashi, N. and Simpson, R.J. (2016) Extracellular vesicle isolation and characterization: toward clinical application. *The Journal of Clinical Investigation*, 126, 1152–1162.
9. Zhao, M., *et al.* (2019) Periodontal ligament fibroblasts regulate osteoblasts by exosome secretion induced by inflammatory stimuli. *Archives of Oral Biology*, 105, 27–34.
10. Wang, Z., Maruyama, K., Sakisaka, Y., Suzuki, S., Tada, H., Suto, M., Saito, M., Yamada, S. and Nemoto, E. (2019) Cyclic stretch force induces periodontal ligament cells to secrete exosomes that suppress IL-1β production through the inhibition of the NF-κB signaling pathway in macrophages. *Frontiers in Immunology*, 10, 1310.
11. Cao, H., *et al.* (2014) Force-induced Adrb2 in periodontal ligament cells promotes tooth movement. *Journal of Dental Research*, 93, 1163–1169.
12. Liu, F., *et al.* (2017) Force-induced H_2S by PDLSCs modifies osteoclastic activity during tooth movement. *Journal of Dental Research*, 96, 694–702.
13. Trajkovic, K., Hsu, C., Chiantia, S., Rajendran, L., Wenzel, D., Wieland, F., Schwille, P., Brügger, B. and Simons, M. (2008) Ceramide triggers budding of exosome vesicles into multivesicular endosomes. *Science*, 319, 1244–1247.

14. Wang, X., *et al*. (2016) Hsp20-mediated activation of exosome biogenesis in cardiomyocytes improves cardiac function and angiogenesis in diabetic mice. *Diabetes*, 65, 3111–3128.
15. Lee, J.S., Kim, S.K., Gruber, R. and Kim, C.S. (2020) Periodontal healing by periodontal ligament fiber with or without cells: a preclinical study of the decellularized periodontal ligament in a tooth replantation model. *Journal of Periodontology*, 91, 110–119.
16. Seo, B.M., *et al*. (2004) Investigation of multipotent postnatal stem cells from human periodontal ligament. *Lancet*, 364, 149–155.
17. Kang, Y.G., Nam, J.H., Kim, K.H. and Lee, K.S. (2010) FAK pathway regulates PGE_2 production in compressed periodontal ligament cells. *Journal of Dental Research*, 89, 1444–1449.
18. Feng, L., *et al*. (2017) Cadherin-11 modulates cell morphology and collagen synthesis in periodontal ligament cells under mechanical stress. *The Angle Orthodontist*, 87, 193–199.
19. Jiang, N., *et al*. (2017) Exosomes mediate epithelium-mesenchyme crosstalk in organ development. *ACS Nano*, 11, 7736–7746.
20. Lobb, R.J., Becker, M., Wen, S.W., Wong, C.S., Wiegmans, A.P., Leimgruber, A. and Möller, A. (2015) Optimized exosome isolation protocol for cell culture supernatant and human plasma. *Journal of extracellular vesicles*, 4, 27031.
21. Menck, K., *et al*. (2017) Neutral sphingomyelinases control extracellular vesicles budding from the plasma membrane. *Journal of extracellular vesicles*, 6, 1378056.
22. Iglesias-Linares, A. and Hartsfield, J.K. Jr (2017) Cellular and molecular pathways leading to external root resorption. *Journal of Dental Research*, 96, 145–152.
23. Davidovitch, Z. and Krishnan, V. (2009) Role of basic biological sciences in clinical orthodontics: a case series. *American Journal of Orthodontics and Dentofacial Orthopedics*, 135, 222–231.
24. Carvalho, C.V., Saraiva, L., Bauer, F., Kimura, R.Y., Souto, M., Bernardo, C.C., Pannuti, C.M., Romito, G.A. and Pustiglioni, F.E. (2018) Orthodontic treatment in patients with aggressive periodontitis. *American Journal of Orthodontics and Dentofacial Orthopedics*, 153, 550–557.
25. Jiang, N., *et al*. (2021) Force-induced autophagy in periodontal ligament stem cells modulates M1 macrophage polarization via AKT signaling. *Frontiers in Cell and Developmental Biology*, 9, 666631.
26. Huang, Y., Liu, H., Guo, R., Han, Y., Yang, Y., Zhao, Y., Zheng, Y., Jia, L. and Li, W. (2021) Long non-coding RNA FER1L4 mediates the autophagy of periodontal ligament stem cells under orthodontic compressive force via AKT/FOXO3 pathway. *Frontiers in Cell and Developmental Biology*, 9, 631181.
27. Zheng, Y., *et al*. (2019) Exosomal microRNA-155-5p from PDLSCs regulated Th17/Treg balance by targeting sirtuin-1 in chronic periodontitis. *Journal of Cellular Physiology*, 234, 20662–20674.
28. Chew, J., Chuah, S.J., Teo, K., Zhang, S., Lai, R.C., Fu, J.H., Lim, L.P., Lim, S.K. and Toh, W.S. (2019) Mesenchymal stem cell exosomes enhance periodontal ligament cell functions and promote periodontal regeneration. *Acta Biomaterialia*, 89, 252–264.
29. Zhao, M., Ma, Q., Zhao, Z., Guan, X. and Bai, Y. (2021) Periodontal ligament fibroblast-derived exosomes induced by compressive force promote macrophage M1 polarization via Yes-associated protein. *Archives of Oral Biology*, 2021, 105263.
30. Pols, M. and Klumperman, J. (2009) Trafficking and function of the tetraspanin CD63. *Experimental Cell Research*, 315, 1584–1592.
31. Cooper, S.M. and Sims, M.R. (1989) Evidence of acute inflammation in the periodontal ligament subsequent to orthodontic tooth movement in rats. *Australian Orthodontic Journal*, 11, 107–109.
32. Kapoor, P., Kharbanda, O.P., Monga, N., Miglani, R. and Kapila, S. (2014) Effect of orthodontic forces on cytokine and receptor levels in gingival crevicular fluid: a systematic review. *Progress in Orthodontics*, 15, 65.
33. Rody, W. J., Jr, Holliday, L. S., McHugh, K. P., Wallet, S. M., Spicer, V. and Krokhin, O. (2014). Mass spectrometry analysis of gingival crevicular fluid in the presence of external root resorption. *American journal of orthodontics and dentofacial orthopedics*, 145, 787–798.
34. Teixeira, C.C., *et al*. (2010) Cytokine expression and accelerated tooth movement. *Journal of Dental Research*, 89, 1135–1141.
35. Bui, T.M., Wiesolek, H.L. and Sumagin, R. (2020) ICAM-1: A master regulator of cellular responses in inflammation, injury resolution, and tumorigenesis. *Journal of Leukocyte Biology*, 108, 787–799.
36. Liu, J., Duan, J., Wang, Y. and Ouyang, X. (2014) Intracellular adhesion molecule-1 is regulated by porphyromonas gingivalis through nucleotide binding oligomerization domain-containing proteins 1 and 2 molecules in periodontal fibroblasts. *Journal of Periodontology*, 85, 358–368.
37. Lee, H.M., Choi, E.J., Kim, J.H., Kim, T.D., Kim, Y.K., Kang, C. and Gho, Y.S. (2010) A membranous form of ICAM-1 on exosomes efficiently blocks leukocyte adhesion to activated endothelial cells. *Biochemical and Biophysical Research Communications*, 397, 251–256.
38. Segura, E., Nicco, C., Lombard, B., Véron, P., Raposo, G., Batteux, F., Amigorena, S. and Théry, C. (2005) ICAM-1 on exosomes from mature dendritic cells is critical for efficient naive T-cell priming. *Blood*, 106, 216–223.
39. He, D., *et al*. (2015) M1-like macrophage polarization promotes orthodontic tooth movement. *Journal of Dental Research*, 94, 1286–1294.
40. Wald, S., *et al*. (2021) γδT cells are essential for orthodontic tooth movement. *Journal of Dental Research*, 100, 731–738.